Instrumentation and Measurement
Technology Conference – IMTC 2007
Warsaw, Poland, May 1-3, 2007

Improvement of the Segmentation by means of the Addition of a Color Vector and the Modeling of the Dispersions of Saturation and Hue

E. Blanco, M. Mazo, L.M. Bergasa, S. Palazuelos and J.C. García
Department of Electronics, University of Alcalá
Alcalá de Henares, 28805, Madrid, Spain
Phone: +34-918856592, Fax: +34-918856591, Email: *{edward, mazo, bergasa, sira, jcarlos}@depeca.uah.es*

Abstract – *In this paper, an alternative that allows to improve the color image segmentation in the HS sub-space (HSI space) is presented. The authors propose to add a color vector in the RGB space with the objective of increasing the separation between classes in the HS plane. This vector is considered optimum and the chromatic C_1C_2 sub-space (YC_1C_2 space) is used to define it. In order to minimize the variances computing times, the authors also propose to estimate the dispersions of the classes projected in the HS plane from their dispersions in the C_1C_2 linear chromatic plane, using the geometric-analytical relationships between both spaces. The proposal presented in this paper has been designed to be applied in real-time on each frame of a color image sequence. Its effectiveness has been tested in applications where a reduced contrast between the background color and the color of the object to segment exists, and when the size of the object to segment is very small in comparison with the size of the captured scene.*

Keywords *– Color segmentation, class separation, HSI space, YC_1C_2 space, mean, dispersion.*

I. INTRODUCTION

From the recent works on color segmentation, S.L. Phung *et al*. [1] segment the skin using a Bayesian classifier, obtaining satisfactory results even under adverse illumination conditions for different color spaces such as: HSV, RGB, YC_bC_r and *CIE-Lab*. R.-L. Hsu *et al*. [2] suggest the detection of face skin, considering a nonlinear subspace of YC_bC_r color space that allows to compensate part of the luminosity variations, and L. Sigal *et al*. [3] use dynamic color models to compensate these variations. About the *HSI* color space, in some works, like [4], a threshold value for the Saturation (*S*) of each pixel based on its Intensity (*I*) is defined. This value is used to determine if *S* should be replaced by Hue (*H*) or by *I* before the clustering process is performed.

In the sign language recognition field, N. Habili *et al*. [5] performed a pixel-by-pixel classification of the skin color with discriminant features of the C_bC_r plane, using the *Mahalanobis distance*, but they need a fusion of motion cues to obtain good results. A similar segmentation is achieved in [6], where post-segmentation process steps have been applied, such as morphological operations, in order to surpass the limitations of the segmentation. In the sign language recognition, it is very important to detect the geometry of the parts to segment (face and hands edges). In order to achieve this, we propose to enhance the contrast between the colors of the object and the background of the scene by means of a pre-process to increase the separation of the classes in the HSI space [7]: we properly color the image with a color vector in the RGB space, taking into account the YC_1C_2 space [8-10]. To obtain the dispersion values of the classes to separate, the authors also propose a modeling (using the geometric-analytical relationships between the HSI and YC_1C_2 spaces) that estimates the hue and saturation deviations in order to reduce the processing time. An estimation of the hue and saturation deviation is performed in [11] for the Smith's HSI transformation.

This paper has been organized as follows: section II presents an introduction about the existing relationships between the YC_1C_2 and HSI spaces, the modeling of the hue and saturation dispersion, and describes the algorithm proposed to increment the separation between classes to improve the segmentation. Section III presents the experimental results, and section IV the conclusions.

II. PROPOSED METHOD

The objective of the proposal presented in this paper is to improve the segmentation process in the HS plane (sub-space where the segmentation should be performed) by adding an optimal color vector to the original image in the RGB space.

A. Algorithm overview

If the original image is denoted by I, the optimal color vector to add by $\mathbf{i_r}$, and the colored image, resulting of the addition by I_i, the following equation is fulfilled:

$$I_i = I + \mathbf{i_r} \tag{1}$$

The determination of the optimal color vector, $\mathbf{i_r}$, is done following the steps shown in Fig. 1. These steps are:
a) From the captured RGB image (I), several (*N*) significant samples (seeds) are obtained from both the object (class O) and the background (class B). i.e., $O_{RGB}=\{\mathbf{r_{O}}_k\}$ and $B_{RGB}=\{\mathbf{r_{B}}_k\}$, for k=1,2,..,*N*.
b) Transformation of the classes O_{RGB} and B_{RGB} from *RGB* space to YC_1C_2 space, resulting: $O_{C1C2}=\{\mathbf{c_{O}}_k\}$ and $B_{C1C2}=\{\mathbf{c_{B}}_k\}$.
c) The optimal location of the classes in the C_1C_2 space is

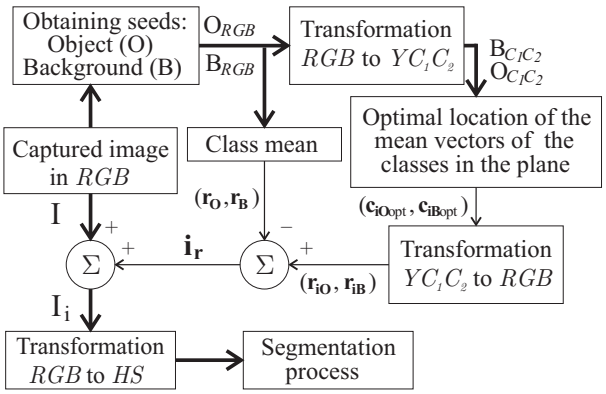

Fig. 1. General block-diagram of the proposed algorithm to obtain the optimal color vector.

obtained by finding the optimal location of their respective mean vectors, $\mathbf{c_{iO}}_{opt}$ and $\mathbf{c_{iB}}_{opt}$.

d) Transformation from YC_1C_2 to RGB of vectors $\mathbf{c_{iO}}_{opt}$ and $\mathbf{c_{iB}}_{opt}$: $\mathbf{r_{iO}}$ and $\mathbf{r_{iB}}$. Using these vectors and the mean vectors of the original classes ($\mathbf{r_O}$ and $\mathbf{r_B}$), the optimal color vector can be calculated:

$$\mathbf{i_r} = \mathbf{r_{iO}} - \mathbf{r_O} = \mathbf{r_{iB}} - \mathbf{r_B} \tag{2}$$

e) Once the optimal color vector has been obtained, the new colored image I_i can be calculated using (1).

Finally, the colored image I_i is transformed from the RGB space to the HS sub-space, where the segmentation is done (HS plane, as in [12]). The color vector $\mathbf{i_r}$ has its effects in the HSI space due to its nonlinearity.

B. Criteria for the separation between classes

We use the Fisher Ratio (FR) to measure the class separability in the HS plane. Due the circular trajectory form of the H component (nonlinear and discontinuous), a particular FR has been considered [13]:

$$FR_H = \theta_h \Big/ \sqrt{\sigma_{HO}^2 + \sigma_{HB}^2}\ ,\ FR_S = \|d_S\| \Big/ \sqrt{\sigma_{SO}^2 + \sigma_{SB}^2} \tag{3}$$

where FR_H and FR_S are the FR of the H and S components, respectively; d_S=μ_{SO}-μ_{SB} is the distance between the saturation means of both classes; σ_{SO}, σ_{SB} and σ_{HO}, σ_{HB} are the standard deviations of the saturation and hue for both classes and θ_h is the separation angle between the hue means of both classes (μ_{HO} and μ_{HB}).

C. Relationships among the RGB, Y C_1C_2 and HSI spaces

Given a vector $\mathbf{r}$=$[R\ G\ B]^T$ (in the RGB space) its components in the YC_1C_2 space [8-10] are given by:

$$\begin{bmatrix} Y \\ C_1 \\ C_2 \end{bmatrix} = \mathbf{Q} \begin{bmatrix} R \\ G \\ B \end{bmatrix};\ \mathbf{Q} = \begin{bmatrix} 1/3 & 1/3 & 1/3 \\ 1 & -1/2 & -1/2 \\ 0 & \sqrt{3}/2 & -\sqrt{3}/2 \end{bmatrix} \tag{4}$$

where $\mathbf{Q}$ is the transformation matrix between spaces. From (4), the C_1 and C_2 components of a vector $\mathbf{c}$=$[C_1\ C_2]^T$ are:

$$C_1 = R - 1/2G - 1/2B\ ,\ C_2 = \sqrt{3}/2G - \sqrt{3}/2B \tag{5}$$

From (5), the phase H' and the module C (Chroma component) of the vector $\mathbf{c}$ in the C_1C_2 plane can be calculated as a function of their RGB values using:

$$H' = \begin{cases} \alpha, B \le G \\ 2\pi - \alpha, B > G \end{cases};\ \alpha = \cos^{-1}\left(\frac{R - 1/2G - 1/2B}{(R^2 + G^2 + B^2 - RG - GB - BR)^{1/2}} \right) \tag{6}$$

$$C = (C_1^2 + C_2^2)^{1/2} = (R^2 + G^2 + B^2 - RG - GB - BR)^{1/2} \tag{7}$$

Therefore, relating the expression of H and S of a vector $\mathbf{h}$=$[H\ S]^T$ in the HSI space [7] with (6) and (7), it can be demonstrated that a vector in the RGB space can be projected in the HS and C_1C_2 planes with the same phase but a different module, i.e., H=H' and $S \neq C$. It can also be demonstrated that the relationship between S and C, knowing that I=Y, is:

$$S = \begin{cases} \dfrac{2C}{3Y}\cos(H - \pi/3) = \dfrac{C_1 + \sqrt{3}C_2}{3Y}; & 0 < H \le 2\pi/3 \\ \dfrac{2C}{3Y}\cos(H - \pi) = -\dfrac{2C_1}{3Y}; & 2\pi/3 < H \le 4\pi/3 \\ \dfrac{2C}{3Y}\cos(H - 5\pi/3) = \dfrac{C_1 - \sqrt{3}C_2}{3Y}; & 4\pi/3 < H \le 2\pi \end{cases} \tag{8}$$

and the relationship between H and the C_1C_2 components, using (5-7), is given by:

$$H = \begin{cases} \delta,\ C_2 \ge 0 \\ 2\pi - \delta,\ \text{otherwise} \end{cases};\quad \delta = \cos^{-1}\left(\frac{C_1}{(C_1^2 + C_2^2)^{1/2}} \right) \tag{9}$$

Therefore, given two mean vectors in the RGB space, as $\mathbf{r_O}$ and $\mathbf{r_B}$, the resulting projection mean vectors in the C_1C_2 ($\mathbf{c_O}$ and $\mathbf{c_B}$) and HS planes ($\mathbf{h_O}$ and $\mathbf{h_B}$) fulfill:

$$\theta_c = \theta_h = \theta, \|\mathbf{c_O}\| \neq \|\mathbf{h_O}\|, \|\mathbf{c_B}\| \neq \|\mathbf{h_B}\| \tag{10}$$

$$\|\mathbf{d_c}\|^2 = g(\mathbf{c_O}, \mathbf{c_B}, \theta_c) = \|\mathbf{c_O}\|^2 + \|\mathbf{c_B}\|^2 - 2\|\mathbf{c_O}\|\|\mathbf{c_B}\|\cos\theta_c \tag{11}$$

where θ_c is the angle between $\mathbf{c_O}$ and $\mathbf{c_B}$, θ_h between $\mathbf{h_O}$ and $\mathbf{h_B}$, and $\mathbf{d_c}$ is the distance vector between $\mathbf{c_O}$ and $\mathbf{c_B}$.

On the other hand, it can be proved that when adding the same vector $\mathbf{i_r}$ (color vector to add) to both $\mathbf{r_O}$ and $\mathbf{r_B}$, the distance vector $\mathbf{d_c}$=$\mathbf{c_O}$−$\mathbf{c_B}$ in the C_1C_2 plane remains constant. This indicates that adding $\mathbf{i_r}$ in the RGB space results in a translation of the classes in the C_1C_2 plane. This effect can be achieved with a translation vector $\mathbf{i_c}$ (corresponding to $\mathbf{i_r}$) directly added in the C_1C_2 plane.

Therefore, the proposed method is based on the analysis of the $\mathbf{c_O}$ and $\mathbf{c_B}$ vectors in the C_1C_2 plane, in the relationships

between the pair of vectors **h** and **c** in the *HS* and C_1C_2 planes, given by (8-11), and in the invariants of $\mathbf{d_c}$ vector: magnitude ($\|\mathbf{d_c}\|$) and phase (ϕ).

D. Separation between the means of hue

The proposed algorithm has been parameterized as a function of the separation angle (θ_i) between the vectors already added with $\mathbf{i_r}$, $\mathbf{c_{iO}}$ and $\mathbf{c_{iB}}$ ("$_i$" indicates that the color vector has been added).

Therefore, if we need that the angle θ_i is maximum, θ_i coincides with the angle whose bisector is a straight line p that passes through the origin of coordinates and is perpendicular to the straight line, m, whose director vector is $\mathbf{d_c}$ (Fig. 2). This implies that the modules of both vectors $\mathbf{c_{iO}}$ and $\mathbf{c_{iB}}$ are equal, i.e., $\|\mathbf{c_{iO}}\|=\|\mathbf{c_{iB}}\|=C_i$ (forced location).

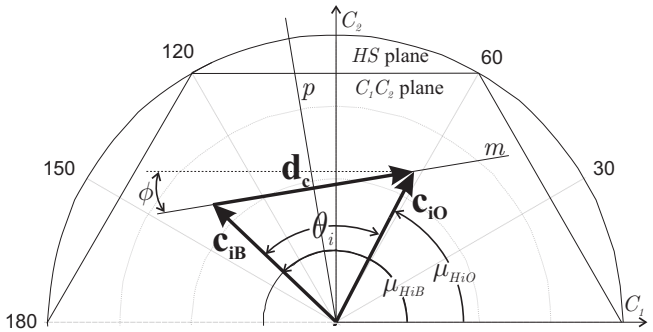

Fig. 2. Location of the vectors $\mathbf{c_{iO}}$ y $\mathbf{c_{iB}}$ in the C_1C_2 plane, once the color vector that produces the forced location has been added.

E. Separation between the means of saturation

In our case, as $\|\mathbf{c_{iO}}\|=\|\mathbf{c_{iB}}\|=C_i$, the difference between the saturation means, $d_S=\|\mathbf{h_{iO}}\|-\|\mathbf{h_{iB}}\|$, as a function of θ_i, depends in great part on the means of the intensities of both classes μ_{IiO} and μ_{IiB} (8). The plane *HS* has three color sectors, (0-2π/3), (2π/3-4π/3) and (4π/3-2π), delimited by the three discontinuities seen in (8), so nine combinations of d_S are possible. For example, if $\mathbf{h_{iO}}$ is located in color sector 1 and $\mathbf{h_{iB}}$ in sector 2 (as Fig. 2 for $\mathbf{c_{iO}}$ and $\mathbf{c_{iB}}$), using (8), we obtain:

$$d_S \simeq (\mu_{C1iO}+\sqrt{3}\mu_{C2iO})/3\mu_{IiO}+\mu_{C1iB}/3\mu_{IiB} \tag{12}$$

where μ_{C1iO}, μ_{C2iO} are the components C_1 and C_2 of vector $\mathbf{c_{iO}}$, and μ_{C1iB}, μ_{C2iB} of the vector $\mathbf{c_{iB}}$.

F. Modeling of the class dispersions

In this paragraph we present the process to estimate the dispersion value of the saturation and hue of the classes, when they are translated in the *HS* plane as a result of the addition of the color vector ($\mathbf{i_r}$). The model estimates the value of the deviation of hue and saturation as a function of the class mean in the C_1C_2 plane, i.e., μ_{C1i} and μ_{C2i}.

1. Modeling of the hue dispersion

The variation of the angular dispersion in the C_1C_2 plane corresponds with the variation of the hue dispersion in the *HS* plane, due to the correspondence between the angle of a vector **c** and a vector **h**, that is the same. A geometric-analytical formulation to relate the hue standard deviation of a class in the *HS* plane with invariant factors of the class for different locations in the C_1C_2 plane is performed. Therefore, the angular deviation or hue deviation (σ_H) can be approximated by half of the angle between the two straight lines tangent to the uncertainty ellipse (one on each side of the angular mean, μ_{Hi}) that also pass through the origin of the C_1C_2 plane. If the class is formed by the vector set: $\mathbf{c}_k=[C_{1k}\ \ C_{2k}]^T$; k=1,2,..,N, the parameters of the uncertainty ellipse of the class (angular invariants, so-called invariants of hue dispersion) are obtained from its covariance matrix. These invariants of hue dispersion are:

$$\omega=\tan^{-1}\left(C_{2u}/C_{1u}\right),\ u=\sqrt{\lambda_u}\ ,\ l=\sqrt{\lambda_l} \tag{13}$$

where ω is the angle of the major axis with respect to the horizontal axis (C_1 axis), u and l are the semimajor and semiminor axes of the ellipse. C_{1u} and C_{2u} are the components of the eigenvector corresponding to the highest eigenvalue (λ_u) of the covariance matrix, and λ_l is the lowest one. The generic equation of an ellipse in the C_1C_2 plane given by:

$$aC_1^2+dC_1+bC_1C_2+cC_2+eC_2^2+f=1 \tag{14}$$

where a, b and c are translation invariant coefficients, because they are only a function of (13), and are given by:

$$a=(\cos^2\omega/u^2+\sin^2\omega/l^2)\ ,\ b=2\sin\omega\cos\omega(1/u^2-1/l^2)\ ,$$
$$c=(\sin^2\omega/u^2+\cos^2\omega/l^2). \tag{15}$$

and d, e and f are translation dependent coefficients, because they are a function of the class mean (μ_{C1i} and μ_{C2i})

$$d=-(2a\mu_{C1i}+b\mu_{C2i})\ ,\ e=-(2c\mu_{C2i}+b\mu_{C1i})\ ,$$
$$f=a\mu_{C1i}^2+b\mu_{C1i}\mu_{C2i}+c\mu_{C2i}^2\ . \tag{16}$$

The estimation of σ_H starts choosing one of the tangency points between the two tangent lines and the ellipse, i.e., $p_t=[C_{1t}\ \ C_{2t}]^T$. Taking the partial derivative of the ellipse equation, knowing that the tangent lines pass through the origin of the plane and the tangency point p_t belongs to the ellipse, C_{1t} can be obtained by:

$$C_{1tj}=\frac{k_1\mathrm{B}\pm\sqrt{k_1(\mathrm{B}^2\text{-}4\mathrm{AC})}}{k_2};\ j=\begin{cases}1;\ +\\ 2;\ -\end{cases} \tag{17}$$

where A=E^2−a/c, B=eb/2c^2−d/c, C=E^2+(1−f)/c, k_1=(1−C/E^2),

k_2=(B^2/2E^2−2A) and E=−e/2c. Then, using (14) and (17), the C_{2t}'s are obtained by means of:

$$(C_{2t11},C_{2t12},C_{2t21},C_{2t22})=\mathrm{E}+\mathrm{D}C_{1tj}\pm\sqrt{\mathrm{A}C_{1tj}^2+\mathrm{B}C_{1tj}+\mathrm{C}} \quad (18)$$

where D=−b/2c. Four tangency points can be obtained from the last equation (18): p_{t1}=(C_{1t1}, C_{2t11}), p_{t2}=(C_{1t1}, C_{2t12}), p_{t3}=(C_{1t2}, C_{2t21}) and p_{t4}=(C_{1t2}, C_{2t22}). All of them may be valid to obtain σ_H, for this reason:

$$\sigma_H=\frac{1}{2}\max\left\{\cos^{-1}\left(\frac{(d_p^2+d_t^2(n)-d_{pt}^2(n)}{2d_pd_t(n)}\right)\right\};\ n=1,2,3 \quad (19)$$

where, with respect to the plane origin, d_p is the distance of the principal point p_p (p_p is the tangency point that produces the largest aperture angle with respect to the mean μ_{Hi}), $d_t(n)$ is the distance of each other point, and $d_{pt}(n)$ is the distance between the principal point and the other tangency points.

Figure 3 depicts the correspondence of a class in both domains HS and C_1C_2. The mean vector **c** of the class in the C_1C_2 plane and its corresponding mean vector **h** of the class in the HS plane are shown. The calculation of the angular or hue deviation (σ_H), by means of the uncertainty ellipse of the class in the C_1C_2 plane, can also be observed.

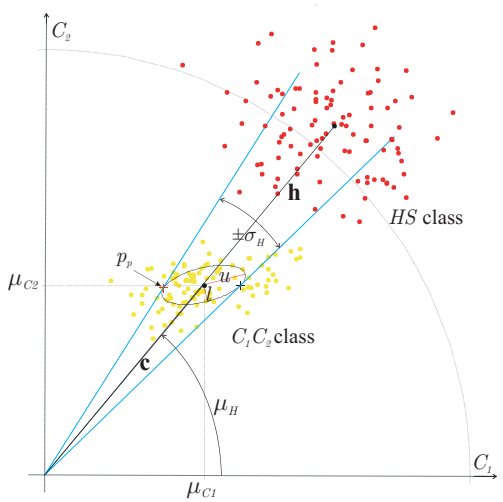

Fig. 3. Correspondence of a class in the C_1C_2 and HS planes. Estimation of the hue deviation by means of the uncertainty ellipse in the C_1C_2 plane.

2. *Modeling of the saturation dispersion*

In this section we demonstrate that it is possible to obtain an expression to model the behavior of the saturation variance of a class when it translates in the HS plane, as a function of μ_{C1i} and μ_{C2i}.

If (8) is substituted in the formula of the saturation variance, in the color sector (0-2π/3), the following equation is obtained:

$$\sigma_S^2=k_N(a_s\mu_{C1i}^2+d_s\mu_{C1i}+b_s\mu_{C1i}\mu_{C2i}+e_s\mu_{C2i}+c_s\mu_{C2i}^2+f_s) \quad (20)$$

where k_N=1/(9N), a_s=(k_1−2k_7/μ_{Ii}), b_s=2$\sqrt{3}a_s$, c_s=3a_s, d_s=2(k_2+$\sqrt{3}k_4$ −k_8/μ_{Ii}−$\sqrt{3}k_9$/μ_{Ii}), e_s=2($\sqrt{3}k_2$ +3k_4−$\sqrt{3}k_8$/μ_{Ii}−3k_9/μ_{Ii}) and f_s=(k_3+2$\sqrt{3}k_5$+3k_6); being k_1=$\mathbf{u}^T(\mathbf{\Sigma}^2)^{-1}\mathbf{u}$, k_2=$\mathbf{u}^T(\mathbf{\Sigma}^2)^{-1}\mathbf{\Delta}$, k_3=$\mathbf{\Delta}^T(\mathbf{\Sigma}^2)^{-1}\mathbf{\Delta}$, k_4=$\mathbf{u}^T(\mathbf{\Sigma}^2)^{-1}\mathbf{\nabla}$, k_5=$\mathbf{\Delta}^T(\mathbf{\Sigma}^2)^{-1}\mathbf{\nabla}$, k_6=$\mathbf{\nabla}^T(\mathbf{\Sigma}^2)^{-1}\mathbf{\nabla}$, k_7=$\mathbf{u}^T\mathbf{\Sigma}^{-1}\mathbf{u}$, k_8=$\mathbf{u}^T\mathbf{\Sigma}^{-1}\mathbf{\Delta}$ and k_9=$\mathbf{u}^T\mathbf{\Sigma}^{-1}\mathbf{\nabla}$; **u** is a Nx1 auxiliary vector formed by 1's, **Δ** is a vector formed by Δ_k={C_{1k}−μ_{C1i}} for k=1, 2… N, **∇** by ∇_k={C_{2k}−μ_{C2i}}, and **Σ** is a diagonal matrix containing the intensities of the vectors. These parameters remain constant in the translation and are called invariants of the dispersion of saturation:

$$\mathbf{\Delta}=[\Delta_1\Delta_2...\Delta_N]^T,\ \mathbf{\nabla}=[\nabla_1\nabla_2...\nabla_N]^T,\ \mathbf{\Sigma}=\begin{bmatrix}I_1 & 0 & \cdots & 0\\ 0 & I_2 & \cdots & 0\\ \vdots & \vdots & \ddots & \vdots\\ 0 & 0 & \cdots & I_N\end{bmatrix} \quad (21)$$

As we can see from (21), **Δ** and **∇** indirectly represent the mean deviations of the components C_1 and C_2 of the class, respectively, and μ_{Ii} =trace(**Σ**)/N.

G. Algorithm to obtain the optimal color vector to add

The algorithm obtains a set of locations of the mean vectors of the classes ($\mathbf{c_{iO}}$ and $\mathbf{c_{iB}}$) in the C_1C_2 plane. Each location is parameterized by the angle θ_i. The optimal value of θ_i, θ_{opt}, is obtained from the set θ_{in} (θ_{i1}, θ_{i2}…) associated to the set of class separation measurement indexes β_{HSn} (β_{HS1}, β_{HS2}…).

The first step of the process is the calculation of the mean vectors of each class, i.e., $\mathbf{c_O}$=E{$\mathbf{c_{O}}_k$} and $\mathbf{c_B}$=E{$\mathbf{c_{B}}_q$}, and, afterwards, the invariants of $\mathbf{d_c}$, given by: $\|\mathbf{d_c}\|$=(d_{C1}^2+d_{C2}^2)$^{1/2}$ and ϕ=cos^{-1}(d_{C1}/$\|\mathbf{d_c}\|$), where [d_{C1} d_{C2}]^T=$\mathbf{c_O}$−$\mathbf{c_B}$. Then, an iterative process is executed, incrementing θ_i by $\Delta\theta$ in each iteration and verifying the validity of the locations of the vectors $\mathbf{c_{iO}}$ and $\mathbf{c_{iB}}$, checking if the component values of the corresponding vectors ($\mathbf{r_{iO}}$, $\mathbf{r_{iB}}$) in RGB space are lower than 1. If the locations are valid, the value of θ_i will be included in the set θ_{in}. For each θ_{in}, the separation between classes is measured with an observation function and registered the pair values θ_{in} and β_{HSn}. Finally, this process obtains θ_{opt} that produces the maximum β_{HSn}. The iterative process includes:

1) Relocation of the original vectors $\mathbf{c_O}$ and $\mathbf{c_B}$ in the C_1C_2 plane (forced relocation), using the invariants ($\|\mathbf{d_c}\|$, ϕ). The Cartesian components particularized for vector $\mathbf{c_{iO}}$, (see Fig. 2), whose angle is: μ_{HiO}=π/2+ϕ −θ_{in} /2, are given by:

$$\mu_{C1iO}=C_i\cos(\mu_{HiO}),\ \mu_{C2iO}=C_i\sin(\mu_{HiO}) \quad (22)$$

2) The translation vector $\mathbf{i_c}$ is obtained for each value of θ_{in}. This $\mathbf{i_c}$ is responsible of the translations of the classes from their original position to the forced location defined by θ_{in}. The classes in the HS plane (O_{iHS} and B_{iHS}) are obtained from the translated classes O_{iC1C2} and B_{iC1C2}, using (8) and (9), and knowing that I=Y.

3) The class separation observation function consists of a normalized measurement index (β_{HSn}) defined from the FR

described in (3), and is given by: $\beta_{HSn}=k_h\beta_{Hn}+(1-k_h)\beta_{Sn}$, where $\beta_{Hn}=(FR_H-1)/FR_H$, $\beta_{Sn}=(FR_S-1)/FR_S$ and k_h is a weighting factor that takes values between 0 and 1. In the calculation of β_{Hn} and β_{Sn} in (3), we have not calculated the dispersion values, but we have used the ones obtained from the modeling proposed in this paper. In the iterative process, the deviation values have been obtained from the following functions: $\sigma_{Hi}=f_H(\omega, u, l, \mu_{C1i}, \mu_{C2i})$ by (13) and $\sigma_{Si}=f_S(\boldsymbol{\Delta}, \boldsymbol{\nabla}, \boldsymbol{\Sigma}, \mu_{C1i}, \mu_{C2i})$ by (21), using only the expressions dependent on the translations.

Once the iterative process has finished, the vector $\mathbf{c_{iO}}_{opt}=[\mu_{C1Oopt} \quad \mu_{C2Oopt}]^T$ (for class O) is obtained from θ_{opt} using (22), and its RGB vector $\mathbf{r_{iO}}=\mathbf{Q}^{-1}[\mu_{YiO}\ \mu_{C1Oopt}\ \mu_{C2Oopt}]^T$, where μ_{YiO} is the mean of the intensity of the class O already translated in the C_1C_2 plane. The $\mathbf{i_r}$ vector is obtained with this $\mathbf{r_{iO}}$ applying (2). In our case, $\mu_{YiO}=\mu_{IO}$, because we want that the mean intensities of the original image (I) and the colored image (I_i) are equal, resulting that $E\{\mathbf{i_r}\}=0$.

The effect obtained in the new image (colored image), I_i, when adding the vector $\mathbf{i_r}$ to the original image, is an equalization of the histogram in H and in S (see Fig. 4).

III. EXPERIMENTAL RESULTS

Practical tests using a bank of real images of different scenes have been carried out to evaluate the effectiveness of the proposed method. Fig. 5 shows an example of the hue and saturation deviation curves calculated (measured) and estimated by means of the proposed modeling for one of the cases of the image bank. The curves for both classes, object (O) and background (B), are shown. Fig. 6 depicts the curves of the real and approximated class separation measurement index β_{HSn} obtained from the calculated and estimated deviations. All these curves are displayed as a function of the angle $\theta_{in}/2$. In the first stage of the tests N=50 samples.

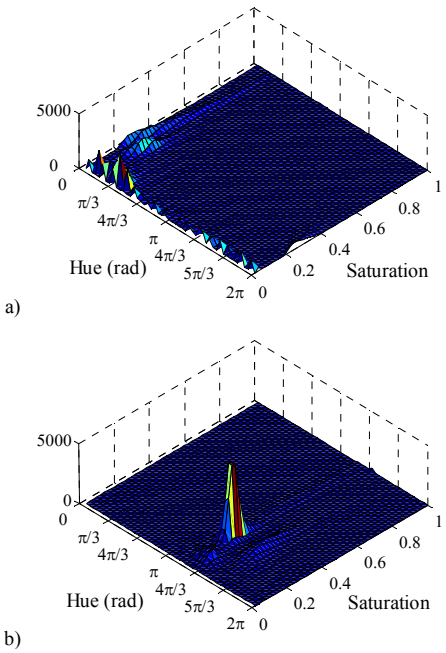

Fig. 4. Example 2D histograms: (a) original image I (b) colored image I_i.

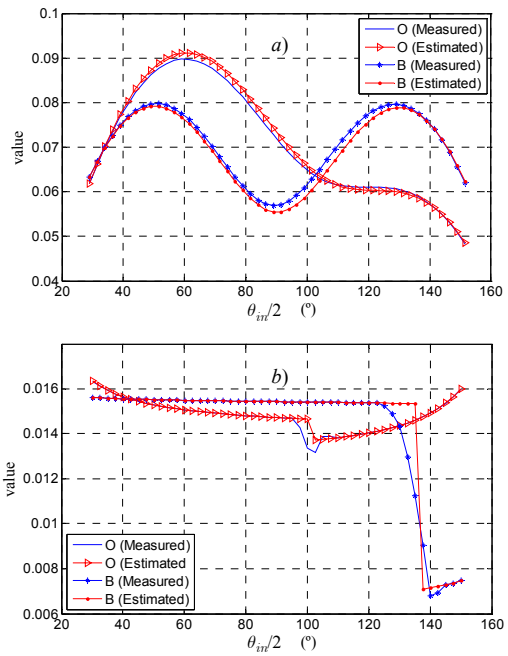

Fig. 5. Measured and estimated deviation curves for a case: a) hue deviations for both classes, b) saturation deviations.

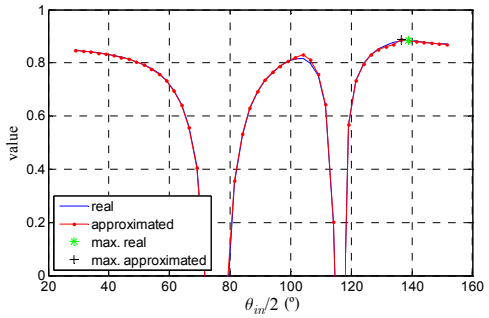

Fig. 6. Class separation measurement index (β_{HSn}), real and approximated, for the Fig. 5 case.

In our tests, the increment in the class separation have been quantified by means of the FR defined in (3), as $FR=FR_H+FR_S$. Table 1 shows the values of FR for 4 cases of the bank of images using $\Delta\theta$=1º and k_h=0.85 in the algorithm.

Table 1. FR results for 4 cases in this work

Case	FR	FR (color vector added)	% increase
1	18.93	35.48	87.40
2	13.72	25.31	84.42
3	2.62	8.62	228.54
4	5.23	10.03	91.57

In order to evaluate the efficiency of the proposed modeling in processing time, diverse tests have been carried out measuring the execution times of iterative process in the algorithm to obtain the optimal color vector to add (paragraph

G of section II). Different number of samples (*N*=50, 100, 200, 500) has been used in these tests, in a PC with Intel Centrino processor at 1.5GHz. In Table 2, the (average) processing times required by the iterative process for the case of Table 1, along with the number of iterations (*M*) are presented. The processing time obtained calculating the variances in each iteration is identified by CPT (variance Calculation Processing Time), and the processing time if the variances are estimated is identified by EPT (variance Estimation Processing Time).

Table 2. Four example CPU times

case	*M*	CPU Times (milliseconds)							
		N=50		*N*=100		*N*=200		*N*=500	
		CPT	EPT	CPT	EPT	CPT	EPT	CPT	EPT
1	49	59.1	19.0	92.2	18.9	180.1	18.9	519.9	19.1
2	37	46.5	15.2	70.9	14.9	131.4	14.8	415.7	15.3
3	59	73.9	21.6	115.6	21.2	215.6	21.3	653.4	21.3
4	46	58.1	17.8	91.4	17.8	170.9	17.6	607.7	17.9

The *Euclidean distance* has been used in the test segmentation process, classifying the pixels according to the minimum distance between the object and background classes. We have utilized such a simple segmentation technique to show the advantages of our proposal. The problems derived from the cyclical nature of the hue in the segmentations have been solved via software.

Four segmentation examples are shown in Fig. 7 (figures a, b, c and d) of the 4 cases of Table 1. Four images are shown for each example, where: the superior left is the original image, the inferior left is the colored image, the right superior shows the segmentation of the original one, and the image of the right inferior part shows the segmentation of the colored image. As it can be observed, our proposal to add a color vector allows to obtain remarkable improvements in the segmentation process.

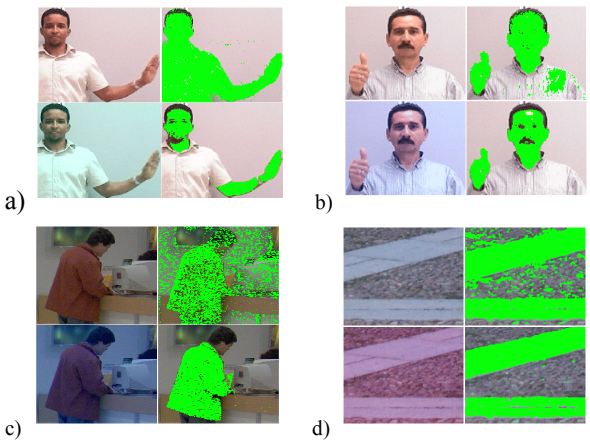

Fig. 7. Results of the segmentation for different persons and objects.

IV. CONCLUSION

A method to improve the segmentation process in *HS* subspace has been proposed. The experimental results obtained demonstrate that adding color to an image guarantees good results in separating the classes and, therefore, better results when segmenting object. We should also take into account that the implementation of our proposal is simple and effective in real-time due to the modeling of the dispersions of *H* and *S*. It has been demonstrated that the proposed modeling of the hue and saturation dispersions has a good accuracy and very low processing times independently of *N*.

It is important to note that the shown images have been obtained directly from the classification process without additional steps, such as morphologic operations.

Currently our research is focused on the addition of a vector $\mathbf{i}_r$ with mean different from 0, and on applying higher order transformations that imply scales and rotations of the classes.

ACKNOWLEDGMENT

The development of these studies has been funded by Ministry of Education and Science (MEC) in the project RESELAI (REF-TIN2006-14896-C02-01).

REFERENCES

[1] S.L. Phung, A. Bouzerdoum and D. Chai, "Skin segmentation using color pixel classification: analysis and comparison", *IEEE Trans. Pattern Analysis and Machine Intelligence*, Vol. 27, Issue 1, pp. 148–154, Jan 2005.

[2] R.-L. Hsu, M. Abdel-Mottaleb and A.K. Jain, "Face detection in color images", *IEEE Trans. Pattern Analysis and Machine Intelligence*, Vol. 24, No. 5, pp.606-706, May 2002.

[3] L. Sigal, S. Sclaroff and V. Athitsos, "Skin color-based video segmentation under time-varying illumination", *IEEE Trans. Pattern Analysis and Machine Intelligence*, Vol. 26, No. 7, July 2004.

[4] S. Sural, Gang Qian and S. Pramanik, "Segmentation and histogram generation using the HSV color space for image retrieval", *Proc. IEEE Int'l Conference Image Processing*, Vol. 2, pp. II–589 – II–592, 22–25 Sept. 2002.

[5] N. Habili, C. C. Lim and A. Moini, "Segmentation of the face and hands in sign language video sequences using color and motion cues",*EEE Trans. Circuits and Systems for Video Technology*, Vol. 14, Issue: 8, pp. 1086–1097, Aug. 2004.

[6] D. Chai and K.N Ngan, "Face segmentation using skin-color map in videophone applications", *IEEE Trans. Circuits and Systems for Video Technology*, Vol. 9, Issue: 4, pp. 551–564, June 1999.

[7] R.C. Gonzalez and R. E. Woods, "Digital image processing", Second Edition, Prentice-Hall Inc., New Jersey, pp. 299, 2002.

[8] T. Carron and P. Lambert, "Color edge detector using jointly hue, saturation and intensity", *Proc. IEEE Int'l Conf. Image Processing*, Vol. 3, pp. 977–981, 13–16 Nov. 1994.

[9] T. Carron and P. Lambert, "Symbolic fusion of hue-chroma-intensity features for region segmentation", *Proc. IEEE Int'l Conf. Image Processing*, Vol. 1, pp. 971–974, 16–19 Sept. 1996.

[10] C. Zhang and P. Wang, "A new method of color image segmentation based on intensity and Hue clustering", *Proc. IEEE 15th Int'l Conf. Pattern Recognition*, Vol. 3, pp. 613– 616, 3–7 Sept. 2000.

[11] S. Romaní, P. Sobrerilla and E. Montseny, "On the Reliability Degree of Hue and Saturation Values of a Pixel for Color Image Classification", *The 14th IEEE International Conference on Fuzzy Systems* FUZZ '05, pp. 306–311, May 22-25, 2005.

[12] X. Zhu, J. Yang and A. Waibel, "Segmenting hands of arbitrary color," *Proc. Int'l Conf. Automatic Face and Gesture Recognition*, pp. 446–453, 2000.

[13] S. Theodoridis and K. Koutroumbas, "Pattern recognition", Academic Press, San Diego, pp. 155–157, 1999.

IMTC/2007®

- Table of Contents
- Message from the Chair
- 2007 Awards
- Technical Sessions
- Author Index

2007 IEEE Instrumentation and Measurement Technology Conference Proceedings

Synergy of Science and Technology in Instrumentation and Measurement

Warsaw Marriott Hotel, Warsaw, Poland, May 1-3, 2007

IEEE Catalog Number: 07EX1720C ISBN: 1-4244-1080-0 Library of Congress: 2007921695

IEEE

IEEE Instrumentation & measurement society

For technical support:
Conference Catalysts, LLC
+1 785 783 5520 – Phone
+1 785 537 3437 – Fax
cdyer@conferencecatalysts.com

Additional copies of this CD may be purchased at:
IEEE Conference Publications Management Group
445 Hoes Lane, Piscataway, NJ 08854
phone: +1 732 562 3872, fax: +1 732 981 1769
e-mail: confpubs@ieee.org

For technical support:
Conference Catalysts, LLC
+1 785 783 5520 – Phone
+1 785 537 3437 – Fax
cdyer@conferencecatalysts.com

IEEE

IEEE instrumentation & measurement society

IMTC/2007®

2007 IEEE Instrumentation and Measurement Technology Conference Proceedings

Synergy of Science and Technology in Instrumentation and Measurement

Warsaw Marriott Hotel, Warsaw, Poland, May 1-3, 2007

8:45AM *Definition of safety performances for an electronic equipment used on rolling stock* [#7305]
Marcantonio Catelani, Lorenzo Ciani, Marco Mugnaini, Valeria Scarano and Roberto Singuaroli
Universita' di Firenze, Italy; Universita' di Siena, Italy

Click here to open the full paper

9:00AM *Employing a Fuzzy Approach to the Fault Diagnosis of Analog Parts of Electronic Embedded Systems* [#7072]
Zbigniew Czaja and Dariusz Zaleski
Gdansk University of Technology, Faculty of ETI, Poland

Click here to open the full paper

9:15AM *Application of the Graph Clustering Algorithm to Analog Systems Diagnostics* [#7396]
Piotr Bilski
Warsaw Agricultural University, Poland

Click here to open the full paper

9:30AM *Analog Neural Network Design for Real-Time Surface Detection with a Laser Rangefinder* [#7170]
Laurent Gatet, Helene Tap-Beteille and Marc Lescure
Electronic Laboratory LEN7 - ENSEEIHT, France

Click here to open the full paper

Special Session Th1d: Measurement Applications of Intelligent Data Processing II

Thursday, May 3, 8:30AM-10:00AM, Room: Ballroom D
Chair: Annamaria R.Varkonyi-Koczy, Fabrizio Russo

8:30AM *Calibration and Error Model Analysis of 3D Monocular Vision Model Based Hand Posture Estimation* [#7286]
Ayman El-Sawah, Nicolas D. Georganas and Emil M. Petriu
Univ. of Ottawa, Canada

Click here to open the full paper

8:45AM *Improvement of the Segmentation by means of the Addition of a Color Vector and the Modeling of the Dispersions of Saturation and Hue* [#7441]
Edward Blanco, Manuel Mazo, Luis Miguel Bergasa, Sira Palazuelos and Juan Carlos Garcia
University of Alcala, Spain

Click here to open the full paper

9:00AM *Gaussian Noise Estimation in Digital Images Using Nonlinear Sharpening and Genetic Optimization* [#7665]
Fabrizio Russo
University of Trieste - D.E.E.I., Italy

Click here to open the full paper